Cooperation of the Conserved Aspartate 439 and Bound Amino Acid Substrate Is Important for High-Affinity Na^+ Binding to the Glutamate Transporter EAAC1

Zhen Tao and Christof Grewer

University of Miami School of Medicine, Miami, FL 33136

The neuronal glutamate transporter EAAC1 contains several conserved acidic amino acids in its transmembrane domain, which are possibly important in catalyzing transport and/or binding of co/countertransported cations. Here, we have studied the effects of neutralization by site-directed mutagenesis of three of these amino acid side chains, glutamate 373, aspartate 439, and aspartate 454, on the functional properties of the transporter. Transport was analyzed by whole-cell current recording from EAAC1-expressing mammalian cells after applying jumps in voltage, substrate, or cation concentration. Neutralization mutations in positions 373 and 454, although eliminating steady-state glutamate transport, have little effect on the kinetics and thermodynamics of Na^+ and glutamate binding, suggesting that these two positions do not constitute the sites of Na^+ and glutamate association with EAAC1. In contrast, the D439N mutation resulted in an approximately 10-fold decrease of apparent affinity of the glutamate-bound transporter form for Na^+, and an ~2,000-fold reduction in the rate of Na^+ binding, whereas the kinetics and thermodynamics of Na^+ binding to the glutamate-free transporter were almost unchanged compared to $EAAC1_{WT}$. Furthermore, the D439N mutation converted L-glutamate, THA, and PDC, which are activating substrates for the wild-type anion conductance, but not L-aspartate, into transient inhibitors of the $EAAC1_{D439}$ anion conductance. Activation of the anion conductance by L-glutamate was biphasic, allowing us to directly analyze binding of two of the three cotransported Na^+ ions as a function of time and $[Na^+]$. The data can be explained with a model in which the D439N mutation results in a dramatic slowing of Na^+ binding and a reduced affinity of the substrate-bound EAAC1 for Na^+. We propose that the bound substrate controls the rate and the extent of Na^+ interaction with the transporter, depending on the amino acid side chain in position 439.

The Journal of General Physiology

INTRODUCTION

Excitatory amino acid carrier 1 (EAAC1) belongs to a family of glutamate transporters (excitatory amino acid transporters, EAATs), which consists of five members (Danbolt et al., 1990; Danbolt et al., 1992; Kanai and Hediger, 1992; Pines et al., 1992; Storck et al., 1992; Fairman et al., 1995; Arriza et al., 1997). The major function of glutamate transporters in the central nervous system is to remove glutamate from the synaptic cleft in order to prevent the glutamate concentration from reaching neurotoxic levels (Zerangue and Kavanaugh, 1996; Tanaka et al., 1997). Glutamate transporters move glutamate from the extracellular space into the cell against its own transmembrane concentration gradient by coupling uphill glutamate transport to the downhill movement of Na^+ and K^+ ions across the membrane (Kanai and Hediger, 1992). The stoichiometry of this coupling is movement of one glutamate$^-$, three Na^+, and one H^+ into the cell and one K^+ out of the cell (Kanner and Bendahan, 1982; Billups et al., 1996; Zerangue and Kavanaugh, 1996; Levy et al., 1998). According to this stoichiometry, glutamate transport is electrogenic and generates current by moving a total of two positive charges to the intracellular side for each transported glutamate ion. Based on the crystal structure of a bacterial glutamate homologue GltPh (Yernool et al., 2004) and from biochemical and physiological studies, the glutamate transporter is a homotrimer (Gendreau et al., 2004) and each subunit works independently (Grewer et al., 2005; Koch and Larsson, 2005).

Glutamate and the cotransported sodium ions bind to specific binding sites on the transporter. Their binding from the extracellular side of the membrane is thought to be a sequential process with at least one Na^+ ion binding to the glutamate-bound form of EAAC1 (Watzke et al., 2001). A highly conserved arginine 446 in transmembrane helix 8 (TM8) of EAAC1 was found to be responsible for coordinating the negatively charged γ-carboxylate group of glutamate (Bendahan et al., 2000; Fig. 1 A). This conclusion was confirmed by the recently published crystal structure of the bacterial

Correspondence to Christof Grewer: cgrewer@med.miami.edu

The online verson of this artical contains supplemental material.

Abbreviations used in this paper: EAAC1, excitatory amino acid carrier 1; EAAT, excitatory amino acid transporter; HEK, human embryonic kidney; PDC, L-*trans*-2,4-pyrrolidine dicarboxcylic acid; RL, reentrant loop; TBOA, DL-*threo*-β-benzyloxyaspartate; THA, D,L-*threo*-β-hydroxyaspartic acid; TM, transmembrane domain.

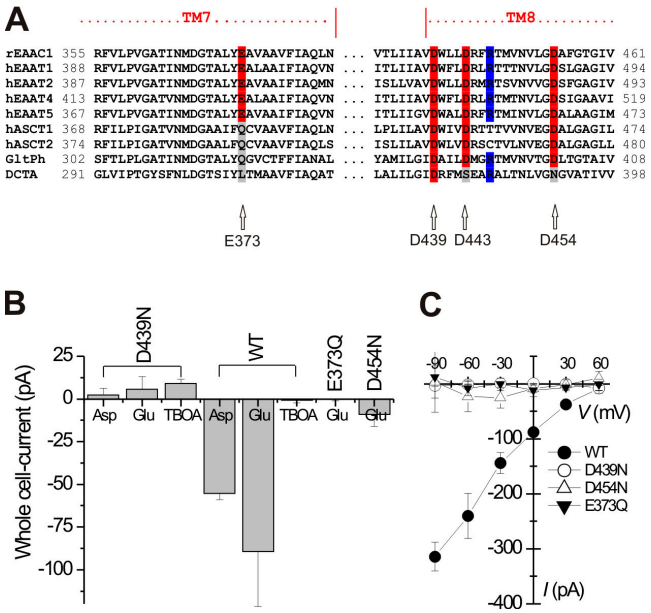

Figure 1. Neutralization of conserved charged amino acid residues in the transmembrane domain of EAAC1 impairs glutamate transport. (A) Sequence alignment of the highly conserved region around charged amino acid residues E373, D439, D443, and D439 (rat EAAC1 numbering) of the EAA and ASC transporters belonging to the SLC1 family. The conserved residues are shown in red, indicated with the arrows. R446, which is responsible for the binding of the γ-carboxylate group of glutamate in EAAC1, is indicated in blue. r and h at the beginning of each line indicate rat or human origin. EAAC, excitatory amino acid carrier; EAAT, excitatory amino acid transporter; ASCT, alanine-serine-cysteine transporter; DCTA, dicarboxylate transporter from *Escherichia coli* O157:H7; GltPh, bacterial glutamate transporter from *Pyrococcus Horikoshii*. (B) Comparisons of transport currents induced by different substrates or an inhibitor (TBOA) between wild-type and mutant EAAC1 proteins. Currents were recorded under forward transport conditions (130 mM KCl in the pipette solution, 140 mM NaCl in the external buffer) with V_{hold} = 0 mV. 1 mM Asp, 10 mM Glu, and 1 mM TBOA were used for $EAAC1_{D439N}$. 100 μM Asp/Glu and 50 μM TBOA were used for $EAAC1_{WT}$. 100 μM Glu was used for $EAAC1_{E373Q}$ and $EAAC1_{D454N}$. (C) Voltage dependence of transport currents of wild-type and mutant EAAC1. Closed circles, $EAAC1_{WT}$; open triangles, $EAAC1_{D454N}$; open circles, $EAAC1_{D439N}$. [Glu] was 100 μM for each experiment.

glutamate transporter homologue GltPh (Yernool et al., 2004), in which excess electron density covered by the tips of reentrant loops (RLs) 1 and 2 and close to the arginine residue analogous to R446 was attributed to a bound substrate molecule. However, in this crystal structure no electron densities accounting for co- or countertransported cations were found, either because the resolution was not sufficient or because the transporter is H^+ instead of Na^+ driven. According to a recent report, the side chain of the aspartate residue D367 in EAAC1 (amino acid numbering throughout this paper is according to the rat EAAC1 sequence, Fig. 1 A) is involved in the binding of Na^+ to the glutamate-free transporter form (Tao et al., 2006). However, it is presently unknown where and how sodium ion(s) interact with the glutamate-bound form of EAAC1.

Acidic amino acid side chains contribute to the coordination of bound Na^+ in a number of Na^+-transporting proteins, such as the Na^+/K^+ ATPase (Jorgensen and Pedersen, 2001) and the bacterial Na^+ ATPase (Meier et al., 2005; Murata et al., 2005). In addition to D367, glutamate transporters have four more conserved acidic amino acid residues in their transmembrane segments (E373, D439, D443, and D454) (Fig. 1 A), possibly contributing to Na^+ binding. Mutations at D443 render the transporter inactive (unpublished data). Therefore, we focused in this study on the other three residues mentioned above (E373, D439, and D454 in TMs 7 and 8 of EAAC1) and tested whether negative charge of these amino acid residues, which are conserved among the mammalian members belonging to the SLC1 (solute carrier 1) family (Fig. 1 A), is required for Na^+ binding to the transporter and carrier function. Although mutagenesis of E373 and D454 had no effect on Na^+ binding to the glutamate-bound transporter, replacement of D439 by neutral, nonionizable amino acid side chains, such as asparagine or serine, strongly decreased the apparent affinity of the substrate-loaded transporter form for Na^+. The D439N mutation also slowed the rate of Na^+ association with its binding site when glutamate was the transported substrate, with a smaller effect on the aspartate-bound form. In contrast, the D to N mutation had only a minor effect on the kinetics and thermodynamics of Na^+ binding to the glutamate-free transporter. In addition, the D439N mutation resulted in a change in the pharmacology of the transporter, converting glutamate, but not aspartate, into a transient inhibitor of the anion conductance. We propose a model for EAAC1 transport in which D439, together with the bound substrate, is involved in controlling the apparent affinity of the glutamate-bound form of the transporter for Na^+ along with controlling the extent and the rate of formation of the anion conducting state.

MATERIALS AND METHODS

Molecular Biology and Transient Expression

Wild-type EAAC1 cloned from rat retina was subcloned into pBK-CMV (Stratagene) as described previously (Grewer et al., 2000) and was used for site-directed mutagenesis according to the QuikChange protocol (Stratagene) as described by the supplier. The primers for mutagenesis were obtained from the DNA core lab, Department of Biochemistry at the University of Miami Miller School of Medicine. The complete coding sequences of mutated EAAC1 clones were subsequently sequenced. Wild-type and mutant transporter constructs were used for transient transfection of subconfluent human embryonic kidney cell (HEK293T/17, American Type Culture Collection number CRL 11268) cultures using FuGENE 6 Transfection Reagent (Roche), according to the supplied protocol. Electrophysiological recordings were performed between days 1 and 3 post-transfection.

Electrophysiology

Substrate induced transporter currents were recorded with an Adams & List EPC7 amplifier under voltage-clamp conditions in the whole-cell current-recording configuration. The typical resistance of the recording electrode was 2–3 MΩ; the series resistance was 5–8 MΩ. Because the currents induced by substrate were small (typically <500 pA), series resistance (R_S) compensation had a negligible effect on the magnitude of the observed currents (<4% error). Therefore, R_S was not compensated. For the experiments in the forward transport mode, the extracellular solution contained (in mM) 140 NaCl, 2 $CaCl_2$, 2 $MgCl_2$, and 30 HEPES, pH 7.3. The pipette solutions contained (in mM) 130 KSCN or KCl, 2 $MgCl_2$, 10 EGTA, and 10 HEPES (pH 7.4/KOH). Thiocyanate was used because it enhances glutamate transporter–associated currents and allows the detection of the EAAC1 anion-conducting mode.

For the electrophysiological investigation of the Na^+/glutamate homoexchange mode the pipette solution contained (in mM) 140 NaCl/NaSCN, 2 $MgCl_2$, 10 EGTA, 10 glutamate, and 10 HEPES (pH 7.4/NaOH). In this transport mode, the same concentrations of Na^+ were used on both sides of the membrane (140 mM). Furthermore, the concentrations of glutamate on the intra- (10 mM) and extracellular side were adjusted to saturate their respective binding site (the exact concentration used depended on the K_m for glutamate of the mutant transporter). According to the nature of the exchange mode it is not associated with steady-state transport current, but only with transient transport current. However, when permeating anions, such as SCN^-, were present, establishment of homoexchange conditions led to the activation of a steady-state anion current (Watzke et al., 2001; Bergles et al., 2002). This steady-state anion current was used in this work as a tool to study the behavior of mutant transporters in the homoexchange mode.

The currents were low pass filtered at 1–10 kHz (Krohn-Hite 3200) and digitized with a digitizer board (Axon, Digidata 1200) at a sampling rate of 10–50 kHz, which was controlled by software (Axon PClamp). All the experiments were performed at room temperature.

Rapid Solution Exchange

Rapid solution exchange was performed as described previously (Grewer et al., 2000). In brief, substrates were applied to the EAAC1-expressing cell by means of a quartz tube (opening diameter: 350 μm) positioned at a distance of ∼0.5 mm to the cell. The linear flow rate of the solutions emerging from the opening of the tube was ∼5–10 cm/s, resulting in typical rise times of the whole-cell current of 30–50 ms (10–90%).

Data Analysis

Nonlinear regression fits of experimental data were performed with Origin (Microcal Software) or Clampfit (pClamp8 Software, Axon Instruments). Dose–response relationships of currents were fitted with a Michaelis-Menten–like equation, yielding K_m and I_{max}. Errors in kinetic parameters are given as standard deviation and were determined from at least four independent experiments from at least three different cells.

Online Supplemental Material

The supplemental material (available at http://www.jgp.org/cgi/content/full/jgp.200609678/DC1) contains five figures. Fig. S1 shows the [Na^+] dependence of the K_m for glutamate and of anion currents induced by saturating glutamate application to $EAAC1_{WT}$ and the various mutant transporters. Fig. S2 shows Western blots to test for cell surface expression of $EAAC1_{D439N}$. Fig. S3 shows the original data for the determination of the K_m for glutamate of $EAAC1_{WT}$ and the various mutant transporters. Control experiments shown in Fig. S4 demonstrate that SCN^- has no irreversible effect on the transporter. Fig. S5 shows original data for $EAAC1_{D439A}$.

RESULTS

Neutralization of Negative Charges in the Transmembrane Domain Eliminates Glutamate Transport

We first tested whether EAAC1 transporters with conservative charge-neutralization mutations in positions 373, 439, and 454 are still able to transport glutamate. As shown in Fig. 1 B, no transport currents were detected upon application of saturating concentrations of glutamate/aspartate to cells expressing transporters with the mutations E373Q and D439N at 0 mV transmembrane potential. Only little steady-state current was observed for $EAAC1_{D454N}$ (<5% of the current measured for $EAAC1_{WT}$, $n = 4$). These results suggest that the glutamate uptake function of EAAC1 is impaired by the replacement of these negatively charged side chains with the neutral amino acid asparagine or glutamine, in agreement with two previous reports on transporters with mutations to the E373 and D439 residues (Pines et al., 1995; Grewer et al., 2003).

Na^+ binding to the empty transporter is known to be voltage dependent (Wadiche et al., 1995). If the charge neutralization mutations would impair a Na^+ binding reaction, it may be possible to restore transport by increasing the driving force for association of Na^+ with the protein by applying more negative membrane potentials. However, even at −90 mV, the transport current induced by glutamate application was negligible (Fig. 1 C), indicating that inhibition of transport by the mutations cannot be overcome by negative membrane potentials.

The D439N Mutation Converts Glutamate from an Activating Substrate to a Transient Inhibitor of the Anion Conductance

Although the mutant transporters show no transport activity, it is possible that some individual reactions in the transport cycle, such as glutamate and Na^+ binding, still take place. To test this possibility, we performed experiments in the anion-conducting mode (KSCN in the intracellular solution). It was shown previously by others and us that mutant transporters without transport activity still catalyze anion current (Bendahan et al., 2000; Seal et al., 2001; Grewer et al., 2003; Tao et al., 2006).

Although we cannot fully exclude the possibility that SCN^-, as a chaotropic ion, can modify the transporter and change the transport kinetics of mutant glutamate transporters, our data show that SCN^- has no irreversible effects on $EAAC1_{WT}$, as well as on $EAAC1_{D439N}$ (see Fig. S4, A and B). These data show that SCN^- neither causes any long-lasting effects, nor permanently activates anion conducting states. Furthermore, we have

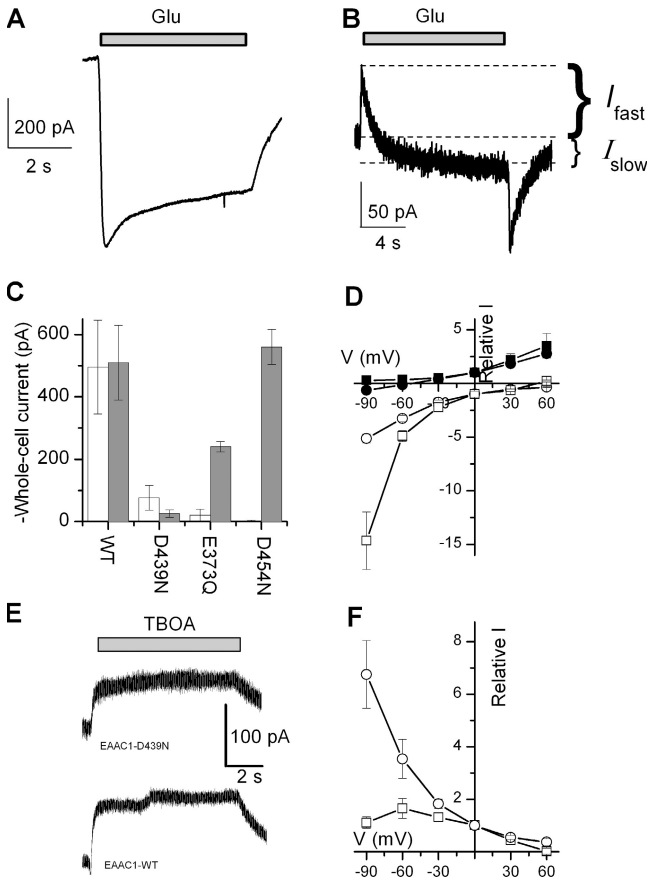

Figure 2. The D439N mutation converts glutamate to a transient inhibitor of the anion conductance. Application of saturating substrate concentrations (100 μM glutamate for $EAAC1_{WT}$ (A) and 5 mM glutamate for $EAAC1_{D439N}$ (B), gray bar) induced anion current in the forward transport mode (130 mM KSCN in the pipette solution, 140 mM NaCl in the external buffer, V_{hold} = 0 mV). The two phases of the current, I_{fast} and I_{slow}, are indicated on the right side. The baseline currents before glutamate application were −390 pA in (A) and −210 pA in (B). (C) Comparison of average whole-cell anion currents induced by saturating substrate (5 mM glutamate for $EAAC1_{D439N}$ and 100 μM glutamate for wild type and other mutants) in the forward transport mode (white bar, solutions as in A) and exchange mode (gray bar, 140 mM NaSCN and 10 mM Glu in the pipette solution, 140 mM NaCl in the external buffer) for wild-type and mutant EAAC1, V_{hold} = 0 mV. (D) Voltage dependence of anion current induced by saturating substrate concentration with the permeable anion SCN^- (130 mM) inside (open symbols) or outside (closed symbols) of the cells (cation concentrations were as in A). Circles, $EAAC1_{D439N}$; squares, $EAAC1_{WT}$. (E) Inhibitory effect of TBOA (1 mM) on the $EAAC1_{WT}$ and $EAAC1_{D439N}$ leak anion currents, 130 mM KSCN as pipette solution, V_{hold} = 0 mV, [NaCl] = 140 mM. (F) The inhibitory effect of TBOA (1 mM) on the leak anion conductance is voltage dependent (open circles). Glutamate (5 mM) induced apparent outward current (see B) is also voltage dependent (open squares). 130 mM KSCN in pipette solution and [NaCl] in the bath was 140 mM.

TABLE I

Comparison of Kinetic Parameters for Mutant and Wild-Type Transporters (Glutamate as Substrate)

	K_m[a] for Glu	I_{max}[b] (exchange)	K_m for Na^+, glutamate free[c]	K_m for Na^+, glutamate bound[d]	τ_{slow}[e]
	μM	pA	mM	mM	ms
E373Q	10 ± 5	−240 ± 20	80 ± 40	7 ± 1	<50
D439N	500 ± 350	−28 ± 7	110 ± 40	100	2600 ± 100
D454N	20 ± 4	−560 ± 60	90 ± 20	7 ± 2	<50
WT	1.4 ± 1	−510 ± 120	120 ± 20	8 ± 1	<50

[a]Apparent affinity for glutamate in the homoexchange mode.
[b]I_{max} was determined at saturating glutamate concentrations in the homoexchange mode.
[c]Apparent affinity of Na^+ to glutamate-free transporter.
[d]Apparent affinity of Na^+ to glutamate-bound transporter.
[e]Time constant of rising phase of the inward current induced by glutamate in the forward transport mode (D439N) or exchange mode (E373Q, D454N, and WT).

shown previously for $EAAC1_{WT}$ that the kinetics of anion current activation and decay correlate with the kinetics of the transport current decay (Watzke et al., 2001). These kinetics also exhibit the same voltage dependence and $[Na^+]$ dependence for the transport and anion current components, suggesting that the anion current is a reliable reporter of transitions in the EAAC1 transport cycle. For these reasons we assume that measurements of anion currents allow us to test whether partial reaction, such as glutamate and Na^+ binding, still take place in mutant transporters.

As shown in Fig. 2 A, large inwardly directed anion currents (−495 ± 150 pA, n = 10) were observed when a saturating concentration (100 μM) of glutamate was applied to $EAAC1_{WT}$-expressing cells at 0 mV transmembrane potential. In contrast, glutamate induced only small steady-state anion currents in $EAAC1_{E373Q}$ and $EAAC1_{D454N}$ ($I < -18$ pA; Fig. 2 C). $EAAC1_{D439N}$ was somewhat in between these two cases, showing an average inward current of −76 ± 40 pA (n = 9; Fig. 2, B and C). Glutamate-induced anion currents measured in all mutant transporters were dose dependent. The apparent K_m values are listed in Table I and the dose–response relationships used to obtain the K_m values are shown in the Fig. S3. Anion currents were also measured in the homoexchange mode (for a detailed explanation see Tao et al., 2006). Although $EAAC1_{E373Q}$ and $EAAC1_{D454N}$ catalyzed large steady-state anion currents in this transport mode, as did $EAAC1_{WT}$ (Fig. 2 C), anion currents carried by $EAAC1_{D439N}$ were small (−27 ± 12 pA, n = 10).

To exclude the possibility of impaired membrane surface targeting of the D439N mutant transporter, we performed surface biotinylation followed by Western blotting. The results from this analysis showed that the $EAAC1_{D439N}$ is expressed in the plasma membrane at levels similar to the wild-type protein (see Fig. S2).

Whereas the anion currents for $EAAC1_{WT}$, $EAAC1_{E373Q}$, and $EAAC1_{D454N}$ in the presence of only intracellular SCN^- were inwardly directed at all conditions tested (SCN^- outflow) and were activated rapidly upon glutamate application ($\tau < 50$ ms), the glutamate-induced

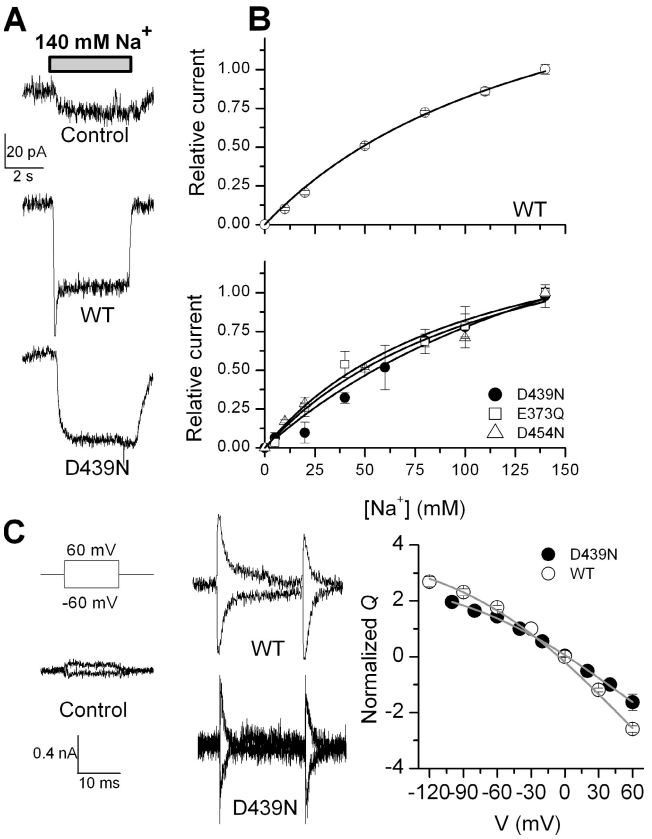

Figure 3. Charge neutralization mutations have no effect on Na^+ binding to the glutamate-free transporter. (A) Anion currents induced by application of 140 mM Na^+ to HEK293 cell transfected with (WT and D439N) or without (Control) transporter cDNA (130 mM KSCN in the pipette solution, 140 mM NaCl in the external buffer V_{hold} = 0 mV). (B) Current–[Na^+] relationships for $EAAC1_{WT}$ (top) and mutant transporters (bottom) determined from raw data as the ones shown in A. The apparent affinities calculated by the fits of a Michaelis-Menten relationship to the data (lines) are listed in Table I. (C) Voltage and time dependence of Na^+ binding to the glutamate-free transporter. HEK293 cells transfected with (WT and D439N) or without (Control) transporter cDNA were initially held at 0 mV, perfused with buffer containing 140 mM NaCl and stepped to −60 or +60 mV for 20 ms, and then repolarized back to 0 mV (see voltage jump protocol in inset). The current shown is the TBOA-sensitive component of the current, obtained by subtraction of the signals in the absence and presence of TBAO (100 μM). The intracellular solution contained 130 mM KCl. The right panel shows the voltage dependence of the normalized charge movement upon stepping the membrane potential (off charge movement). The lines represent calculations according to the Boltzmann equation with z_Q = 0.35 and $V_{1/2}$ = 48 mV.

current catalyzed by $EAAC1_{D439N}$ showed peculiar biphasic behavior (Fig. 2 B). At short times after application of 5 mM glutamate, a rapid outward component of the current was observed (I_{fast}), which was followed by a slow development of an inwardly directed component (I_{slow}, Fig. 2 B, time constant indicated by τ_{slow}). The formation of the outward current component was instantaneous within the time resolution of the solution exchange system used (50–80 ms). The formation of the inward component took place with a time constant of τ_{slow} = 2,600 ± 700 ms (n = 18, KSCN as pipette solution). Upon removal of glutamate, an initial, inwardly directed overshoot of the current over the steady-state level was observed. Subsequently, the current decayed slowly (τ = 4,900 ± 1,800 ms, n = 15) to the baseline level. Due to the unusual kinetic behavior of $EAAC1_{D439N}$ and the wild-type–like kinetic behavior of $EAAC1_{E373Q}$ and $EAAC1_{D454N}$, the following experiments focused mostly onto the more detailed investigation of $EAAC1_{D439N}$.

The voltage dependence of the steady-state anion current of $EAAC1_{D439N}$ is shown in Fig. 2 D in comparison with the $EAAC1_{WT}$ data. In the presence of SCN^- only on the intracellular side the current is inwardly directed at all membrane potentials (−90 to +60 mV), as in wild-type EAAC1. As expected for a purely anion-selective membrane, the current is outwardly directed in the presence of SCN^- only on the extracellular side. In contrast to $EAAC1_{WT}$ current, which reverses direction at about −50 mV (Fig. 2 D), current carried by $EAAC1_{D439N}$ does not reverse, due to the absence of a transport current component. These data show that the current carried by $EAAC1_{D439N}$ is a pure anion current.

The outward current, I_{fast}, induced by glutamate application to $EAAC1_{D439N}$ in the presence of only intracellular SCN^- is most likely caused by inhibition of a tonic SCN^- leak current. In wild-type EAAC1, the application of competitive inhibitors, such as DL-*threo*-β-benzyloxyaspartate (TBOA), generates outward current under similar ionic conditions (Fig. 2 E; Shimamoto et al., 1998; Grewer et al., 2000). Consistent with this, TBOA also generated outward current in $EAAC1_{D439N}$-expressing cells (Fig. 2 E). This outward current had the typical voltage dependence expected, increasing at more negative potentials, and was generally similar to the voltage dependence of the glutamate-induced anion current measured at the peak of the outward current response (Fig. 2 F). However, the glutamate-induced outward current, I_{fast}, showed weaker voltage dependence than that induced by TBOA, most likely caused by the limited time resolution of our solution exchange method. At very negative potentials, the rise of I_{slow} becomes very fast, so much that the measured peak response of I_{fast} is smaller than the real peak response because I_{slow} starts being activated during the time required for the solution exchange. Together, these results show that the charge neutralization in position 439 converts glutamate into a transient inhibitor of the glutamate transporter leak anion conductance. Furthermore, at least one reaction in the transport cycle is dramatically slowed by this mutation. Our next aim was to determine which step(s) in the transport cycle is (are) slowed by the D439N amino acid exchange to cause its anomalous behavior.

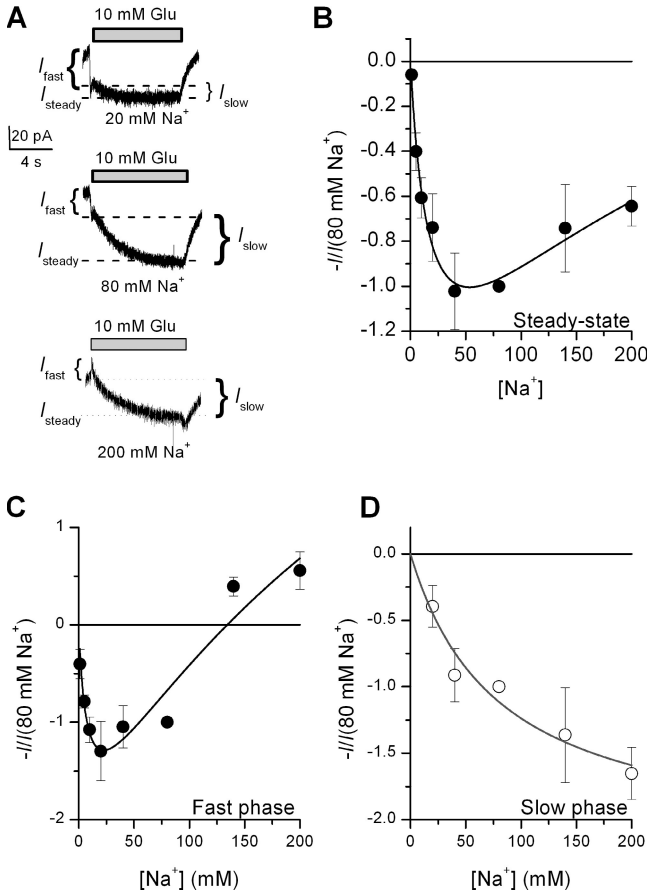

Figure 4. Direct and separate observation of two Na^+ binding processes spread out on the time scale in $EAAC1_{D439N}$. (A) Anion currents induced by application of 10 mM glutamate to $EAAC1_{D439N}$ at 20 mM (top), 80 mM [Na^+] (middle), and 200 mM [Na^+] (bottom) under exchange conditions (140 mM NaSCN, 10 mM glutamate in pipette solution, the external anion was Cl^-, 140 mM, V_{hold} = 0 mV). I_{fast} denotes the rapidly rising outward current at the beginning of each trace; I_{steady} is steady-state current; I_{slow} is the inwardly directed current for the slow rising phase. The relationships of each of these current components to [Na^+] are shown in B (I_{steady}-[Na^+] relationship), C (I_{fast}-[Na^+] relationship), and D (I_{slow}-[Na^+] relationship). The solid lines in B and C represent fits to Eqs. 2 and 3, respectively (Appendix) with parameters G_{TNa} = 1.2, G_{TNaS} = 0.5, G_{TNa2S} = 1, K_{N1} = 110 mM, K_{N2} = 300 mM, and K_S = 500 μM (see also Fig. S1). The results of simulations used to estimate the kinetic parameters of Na^+ binding are shown in Fig. 7 C. The solid line in D represents a fit of the Michaelis-Menten kinetics to the data with a K_m of 80 ± 28 mM.

The Kinetics of Na^+ Binding to the Glutamate-free Transporter Form Are Not Affected by the D439N Mutation

The apparent affinity of the glutamate-free EAAC1 for Na^+ was determined by recording leak anion currents induced by different extracellular [Na^+] as detailed in Tao et al. (2006). Original data are shown in Fig. 3 A. Na^+-induced anion currents were observed in EAAC1 wild type and $EAAC1_{D439N}$-transfected cells, but only to a small extent in control-nontransfected cells (Tao et al., 2006). These anion currents were [Na^+] dependent and showed saturation behavior with K_m values of 120 ± 20 mM and 110 ± 40 mM, respectively (Fig. 3 B, Table I). The K_m values for this Na^+ binding step for $EAAC1_{E373Q}$ and $EAAC1_{D454N}$ are also listed in Table I and were identical to the wild-type value, within experimental error. Whereas $EAAC1_{WT}$, $EAAC1_{E373Q}$, and $EAAC1_{D454N}$ showed purely Michaelis-Menten–like [Na^+]–current relationships, $EAAC1_{D439N}$ showed sigmoidal dose–response behavior (Fig. 3 B). The reason for this behavior is not known. However, it may be possible that two Na^+ ions bind to the transporter in the absence of glutamate, thus giving rise to cooperativity of Na^+ binding. Although including a second Na^+ association step into our model can fit this particular result obtained for $EAAC1_{D439N}$ well, our data presented here overall do not allow us to rigorously differentiate whether one or two Na^+ ions bind to the glutamate-free transporter; this point will be addressed elsewhere. To determine the rate of Na^+ binding to the empty transporter, we performed voltage jump experiments, as shown in Fig. 3 C (middle). Like in $EAAC1_{WT}$, step changes in the membrane potential induced a transient capacitive current in $EAAC1_{D439N}$-expressing cells. For the wild-type transporter, these transient currents were proposed to be caused by electrogenic binding of Na^+ to the glutamate-free transporter (Wadiche et al., 1995). The time constant of the decay of the transient currents in $EAAC1_{D439N}$ was ∼1.0 ± 0.2 ms (n = 5) and, like in wild-type EAAC1, it was nearly voltage independent (the τ value for $EAAC1_{WT}$ was 0.88 ± 0.06 ms). The voltage dependence of the voltage jump–induced charge movement, Q, is shown in Fig. 3 C (right). For both $EAAC1_{WT}$ and $EAAC1_{D439N}$ Q began to saturate when jumping the potential to very negative values, as expected for the saturation of the Na^+ binding site of the empty transporter at these potentials. Both Q-V relationships could be represented using the same parameters (apparent valence, z_Q = 0.35, $V_{1/2}$ = 48 mV), consistent with similar K_m values for Na^+ of both transporters. Together, these data indicate that the kinetics and thermodynamics of Na^+ binding to glutamate-free $EAAC1_{D439N}$ are almost unchanged compared with the wild-type transporter and cannot account for the unusual anion currents found in this mutant transporter.

The Kinetics of Na^+ Binding to the Glutamate-bound Transporter Form Are Strongly Affected by the D439N Mutation

Binding of Na^+ to the glutamate-loaded transporter can be observed in isolation under conditions of saturating glutamate concentrations by analyzing the [Na^+] dependence of glutamate-induced steady-state anion currents (I_{steady}; Watzke et al., 2001). By performing such experiments in the homoexchange mode, $EAAC1_{E373Q}$ and $EAAC1_{D454N}$ showed Na^+ dose–response

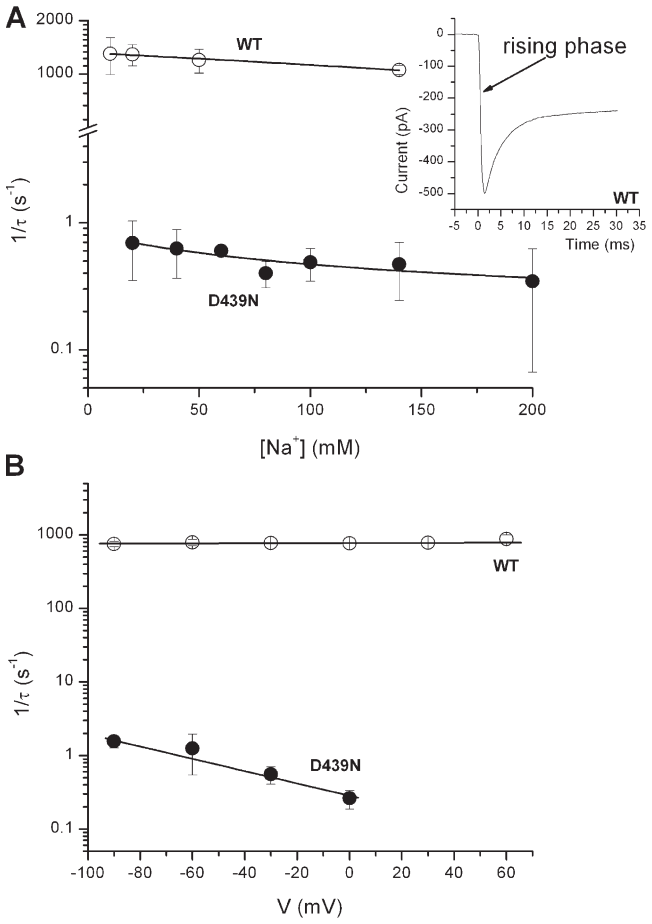

Figure 5. Comparison of the relaxation rate constants for the slow rising phase (I_{slow}) for $EAAC1_{D439N}$ and the rising phase for $EAAC1_{WT}$ glutamate-induced anion currents. (A) Rate constant–$[Na^+]$ relationships for $EAAC1_{WT}$ (open circles) and $EAAC1_{D439N}$ (closed circles). The solid line for $EAAC1_{D439N}$ represents the result of a fit of the $\log(1/\tau)$ versus $[Na^+]$ relationships according to Eq. 1, Appendix, with parameters $k_1 = 0.25\ s^{-1}$, $k_{-1} = 0.5\ s^{-1}$, and $K_{N2} = 80$ mM. For $EAAC1_{WT}$ the line was drawn to guide the eye. The inset shows a typical trace induced by glutamate released from 1 mM MNI-Glu by laser (130 mM KSCN in pipette solution, the external anion was Cl^-, 140 mM). The rising phase is indicated by arrow. (B) Rate constant–voltage relationships for $EAAC1_{WT}$ (open circles) and $EAAC1_{D439N}$ (closed circles). The solid lines represent the results of a linear regression analysis of the $\log(1/\tau)$ versus V_{hold} relationships with slopes of 9×10^{-5} mV^{-1} ($EAAC1_{WT}$) and $-8 \times 10^{-3}\ mV^{-1}$ ($EAAC1_{D439N}$). The ionic conditions were as in A.

relationships with K_m values very similar to the wild-type transporter (Table I and Fig. S1), indicating that these two charge neutralization mutations did not affect Na^+ binding to the glutamate-bound form of EAAC1. In contrast, $EAAC1_{D439N}$ showed a different behavior, as illustrated in Fig. 4 (A and B). At steady state, the inward anion current was not representative of a simple Michaelis-Menten–type dose–response relationship, but decreased with increasing Na^+ concentrations after initially increasing at low $[Na^+]$ to reach a maximum at ~50 mM Na^+ (Fig. 4 B). This $[Na^+]$–response relationship with two clear components directly shows that at least two Na^+ ions bind separately to EAAC1. In the next paragraphs, these two Na^+ binding processes will be dissected in detail.

In addition to the steady-state current, the time dependence of the anion current was modulated by external $[Na^+]$ (Fig. 4 A). At low sodium concentrations (20 mM), no fast outward current component was observed, but a fast phase of the current was inwardly directed and dominated the total current. As the $[Na^+]$ was increased, the fast inward phase of the current (I_{fast}) decreased, whereas the slow component (I_{slow}) became more pronounced. This opposite Na^+ concentration dependence of I_{fast} and I_{slow} is summarized in Fig. 4 (C and D). At high $[Na^+]$ (>120 mM), I_{fast} eventually becomes outwardly directed (Fig. 4, A and C). At very low $[Na^+]$ (<20 mM), I_{fast} decreases due to nonsaturation of the glutamate binding site at the glutamate concentration of 10 mM used in these experiments (see also Fig. S1 C, for data on the $[Na^+]$ dependence of the K_m for glutamate). The decrease of I_{fast} with increasing $[Na^+]$ suggests that glutamate acts as a partial inhibitor of the Na^+-induced leak anion conductance of the glutamate-free transporter. The $[Na^+]$ dependence of this current component will be quantitatively described in the Discussion.

In contrast to I_{fast}, the slow, inwardly directed component of the current increased with increasing $[Na^+]$ (Fig. 4 D), suggesting that it is associated with a different Na^+ binding process. The apparent K_m for $[Na^+]$ of this component was determined from a simple Michaelis-Menten fit to 80 ± 28 mM. In the Discussion, this current component will be assigned to the Na^+ binding step to the glutamate-bound form of EAAC1.

In the wild-type transporter, the time constant of the rising phase of the anion current induced by rapid application of glutamate released from caged glutamate by laser pulse photolysis (see inset in Fig. 5) is independent of the Na^+ concentration (Fig. 5 A, open circles). This observation led to the proposal that the actual Na^+ binding process is rate limited by a slow, preceding structural change in the transporter making it competent for subsequent fast binding of Na^+ (Watzke et al., 2001). Consistently, $1/\tau_{slow}$ (Fig. 2 B) of $EAAC1_{D439N}$ was also virtually independent of the extracellular $[Na^+]$ (Fig. 5 A, closed circles). This would not be expected if Na^+ binding was rate limiting or if fast Na^+ binding would precede a slow structural change. However, the finding would be consistent with a slow, glutamate-induced structural change preceding fast Na^+ binding. In fact, $1/\tau_{slow}$ was [glutamate] dependent, increasing from 0.6 ± 0.3 s^{-1} at 1 mM glutamate to 1.5 ± 0.2 s^{-1} at 10 mM glutamate (unpublished data). The $1/\tau_{slow}$ versus $[Na^+]$ relationship of $EAAC1_{D439N}$ can be quantitatively described by Eq. 1 (Appendix), according to the model described in the Discussion section.

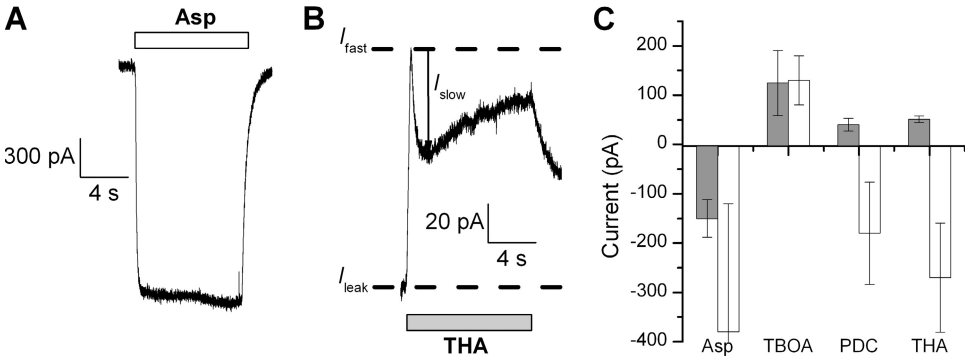

Figure 6. The D439N mutation changes the pharmacology of the transporter substrate binding site. (A) Anion current induced by application of 1 mM aspartate at 140 mM external NaCl to $EAAC1_{D439N}$ under exchange conditions (140 mM NaSCN, 10 mM glutamate in pipette solution), V_{hold} = 0 mV. (B) Similar experiment as in A but with 1 mM THA as substrate and [Na^+] was 400 mM, exchange mode, V_{hold} = 0 mV. I_{leak}, anion leak current induced by Na^+ binding to glutamate-free form transporter; I_{fast}, apparent outward current at the beginning of the trace at t = 0; I_{slow}, inward current slowly developing from the I_{fast} level as indicated by the arrow. (C) Comparison of steady-state anion currents induced by different substrates/inhibitors in $EAAC1_{WT}$ (blank bars) and $EAAC1_{D439N}$ (gray bars) under exchange conditions, V_{hold} = 0 mV.

We also determined the voltage dependence of $1/\tau_{slow}$, as shown in Fig. 5 B. Whereas $1/\tau_{slow}$ was not voltage dependent in the wild-type transporter, we found a significant voltage dependence for $EAAC1_{D439N}$. The $\log(1/\tau_{slow})$ versus voltage relationship of the mutant transporter had a slope of -8×10^{-3} mV^{-1}, whereas that of $EAAC1_{WT}$ was 9×10^{-5} mV^{-1}. The changed voltage dependence of the anion current rising phase of $EAAC1_{D439N}$ is not surprising, given the neutralization of a putative negative charge in the membrane domain.

The Kinetics of Na^+ Binding to $EAAC1_{D439N}$ Depend on the Nature of the Transported Substrate

The data obtained so far indicate that glutamate is a partial substrate of $EAAC1_{D439N}$. To further characterize the functional effects of the mutation, we tested activation of the anion conductance by substrates other than glutamate. These experiments were performed in the anion-conducting mode in the presence of 140 mM intracellular SCN^-. When L-aspartate was applied to $EAAC1_{D439N}$, steady-state inward anion currents were generated (Fig. 6 A) with an average amplitude of -150 ± 40 pA (Fig. 6 C). In contrast to the slow anion current activation by glutamate, this aspartate-activated anion current rose rapidly with an average time constant of 140 ± 70 ms. The kinetics of this current rise were limited by the time resolution of the solution exchange system used. Thus, the real rise time of the current could be faster. The kinetic parameters of the activation of the anion current by L-aspartate in comparison to glutamate are summarized in Table II. Although the anion current induced by aspartate in $EAAC1_{D439N}$ is only ~40% of that induced by aspartate in the wild-type transporter (Fig. 6 C), the kinetic properties were generally wild-type like. For example, the current didn't show the characteristic transient outward phase observed after binding of glutamate to $EAAC1_{D439N}$.

The data obtained with aspartate as the substrate suggested that the kinetics of anion current activation in $EAAC1_{D439N}$ depend strongly on the nature of the bound substrate. To test this hypothesis, we determined the effects of two other substrates, L-*trans*-2,4-pyrrolidine dicarboxcylic acid (PDC) and D,L-*threo*-β-hydroxyaspartic acid (THA), on the anion current properties of the transporter. Application of these substrates to $EAAC1_{WT}$ at a concentration of 1 mM induced inward anion currents (Fig. 6 C). In contrast, these two substrates induced outward currents in $EAAC1_{D439N}$-expressing cells (Fig. 6, B and C), indicating that they act as inhibitors of the leak anion conductance. The outward current induced by THA application showed a transient outward peak, I_{fast}, developing within the time course of the solution exchange, which was followed by a slower decay with the amplitude I_{slow} to a steady-state current level (the second slow rise seen in the particular trace shown is most likely not significant because we did not observe it in all experimental traces). This decay occurred with a time constant of 260 ± 6 ms. This behavior is reminiscent of that described above for glutamate as the

TABLE II

Comparison of Steady-State Kinetic Parameters of D439N Activation by Substrates/Inhibitors

	K_m of substrate/ inhibitor[a]	I_{max}[b] (exchange mode)	K_m for Na^+, substrate-bound[c]	τ_{slow}[d]
	μM	pA	mM	ms
L-Glu	500 ± 350	−28 ± 7	>300	2,600 ± 700
L-Asp	100 ± 20	−150 ± 40	90 ± 40	140 ± 70
TBOA	3 ± 1	63 ± 37	–	–

[a]Apparent affinity for substrate/inhibitor in the exchange mode.
[b]I_{max} was determined at saturating glutamate concentrations in the exchange mode.
[c]Apparent affinity of Na^+ to glutamate-bound transporter.
[d]Time constant of rising phase induced by L-glutamate or L-aspartate in the forward transport mode.

substrate, except that in the case of THA the substrate-induced inward current (I_{slow}) did not exceed the baseline inward current (I_{leak}) measured before THA application (Fig. 6 B).

DISCUSSION

The stoichiometry of the coupling of glutamate transport to the cotransported sodium ions of the glutamate transporter subtypes EAAT3 and Glt1 was shown to be 1:3 (Zerangue and Kavanaugh, 1996). Although the stoichiometry of rat EAAC1 has not been determined experimentally, it is likely to be identical to human EAAT3, based on the 96% sequence similarity between the two proteins. Here, we demonstrate the direct observation of the association of two of these three cotransported Na^+ ions with the transporter. In the wild-type transporter these association reactions occur on a submillisecond time scale and are, therefore, difficult to study. Charge neutralization mutations to position D439, but not E373 and D454, slow the association of Na^+ with the glutamate-bound form of the transporter significantly (~2,000 fold, Fig. 2), while leaving the rate of interaction of Na^+ with the glutamate-free transporter form essentially unchanged (Fig. 3). Thus, binding of the two Na^+ ions is spread out on the timescale. The D439N mutation also decreases the apparent affinity of the glutamate-bound transporter for Na^+ ~10-fold (Fig. 4), whereas the E373Q and D454N mutations have a negligible effect on this affinity (Fig. S1). Therefore, we conclude that the latter two negatively charged amino acids are not involved in binding of Na^+ by the glutamate-bound transporter, since their neutralization had essentially no effects on binding properties of the substrate, cotransported ions, and translocation properties, as assayed in the homoexchange mode. It is rather likely that these two mutations, which both eliminate steady-state glutamate transport, affect the K^+-dependent branch of the transport cycle. Charge neutralization mutations in position E373 were previously shown to eliminate the K^+-induced relocation reaction (Kavanaugh et al., 1997), but not K^+ binding to the transporter (Grewer et al., 2003). Therefore, it is likely that E373 is only important for protonation of EAAC1, as proposed recently (Grewer et al., 2003), but not for binding of the cotransported Na^+ ions and countertransported K^+ ions.

We have previously shown that out of the three cotransported Na^+ ions at least one associates with the empty transporter and at least one associates with the glutamate-bound form of EAAC1 (Watzke et al., 2001). Whether the third Na^+ binds to the empty transporter, to the glutamate-bound form, or both of these forms is unclear and the current data do not allow us to precisely differentiate between these possibilities. The sigmoidicity of the $[Na^+]$–current response curve of $EAAC1_{D439N}$ (Fig. 3 B) suggests association of the third Na^+ with the glutamate-free transporter form, but this point needs further clarification by future experiments. Although association of Na^+ with the empty transporter and the apparent affinity for this process can be measured experimentally, binding of substrate and Na^+ must necessarily be coupled to achieve concentrative uptake of substrate driven by the $[Na^+]$ gradient, thus leading to a modulation of the Na^+ affinity by substrate binding. This modulation behavior is predicted by the model shown in Fig. 7 A. Glutamate binding to the "empty" transporter with only Na^+ bound will increase the apparent affinity of the transporter for this/these Na^+ ion(s), resulting in locking-in of Na^+ to the binding site(s) at saturating glutamate concentrations.

Negative Charge in Position 439 Is Not Required for Na^+ Binding, but its Neutralization Changes Na^+ Binding Properties of the Glutamate-bound Transporter

Since the D439N mutation dramatically alters the kinetics and thermodynamics of Na^+ binding to the glutamate-bound form of EAAC1, the acidic D439 side chain may be directly involved in Na^+ coordination. Although this is a possibility that we cannot fully exclude based on our data, it is more likely that the effect of the D439N mutation on Na^+ binding is indirect for the following reasons. (a) Mutation to alanine, which is less conservative than the mutation to asparagine, does not fully abolish Na^+ binding. In fact, Na^+ binds with relatively high apparent affinity (K_m ~30 mM) to the aspartate-bound form of $EAAC1_{D439A}$ (Fig. S5). (b) The aspartate-bound $EAAC1_{D439N}$ transporter binds Na^+ with an apparent affinity and kinetics similar to those of the wild-type transporter. (c) In the crystal structure of the glutamate transporter homologue, GltPh, the residue analogous to D439 is localized close to the extracellular surface of the protein (Fig. 7 B). In most ion-translocating membrane proteins crystallized so far, cation binding sites were found closer to the center of the hydrophobic core of the protein (Toyoshima and Inesi, 2004). If the Na^+ binding site was, in fact, close in space to D439, it is difficult to envision how this ion could be translocated to the trans side of the membrane from this position. (d) It was proposed previously that Na^+ binding to the glutamate-bound transporter is associated with transmembrane charge movement (Watzke et al., 2001), suggesting that Na^+ access to its binding site is through part of the membrane electric field (one charge moving through 60% of the electric field). Because of its localization close to the extracellular surface in the GltPh structure (Fig. 7 B), it appears unlikely that a charge moving to D439 would sense much, if any, of the membrane electric field. (e) The rate of the current rise (slow phase, $1/\tau_{slow}$) is independent of the extracellular Na^+ concentration (Fig. 5 A). Because the amplitude of the slow phase is strongly dependent on $[Na^+]$,

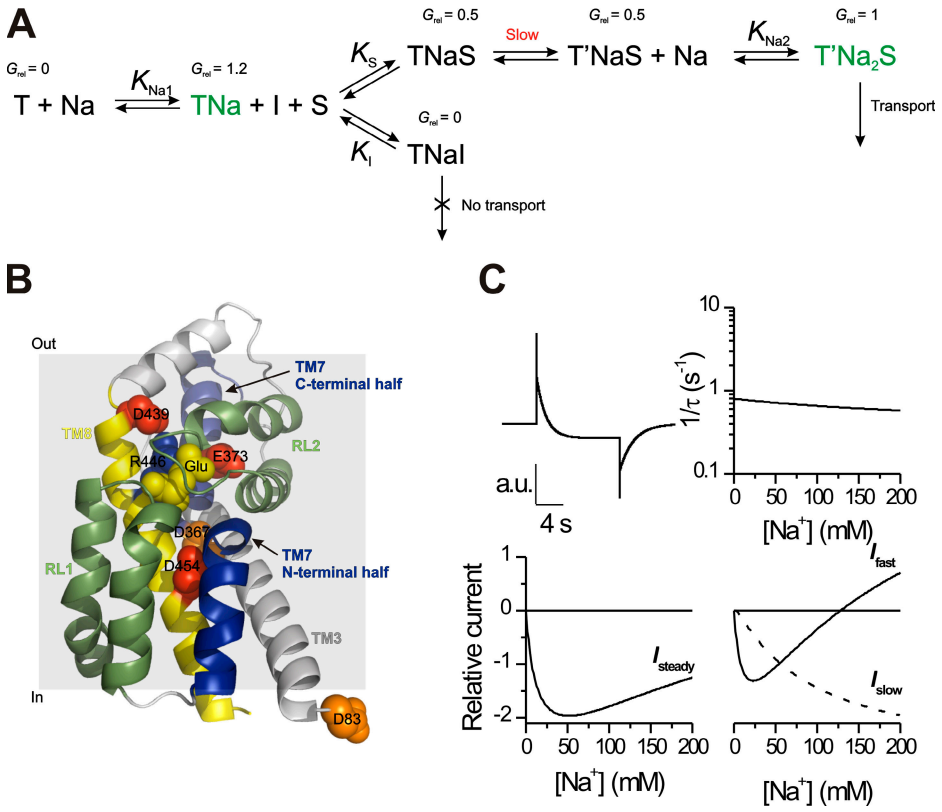

Figure 7. (A) Kinetic model for $EAAC1_{D439N}$. T, transporter; I, inhibitor; S, substrate; K_x, dissociation constant for the corresponding reaction step; G_{rel}, relative conductance of individual transporter state to the fully loaded transporter state, $T'Na_2S$. (B) Simplified ribbon representation of TM3 (gray) and the C-terminal segment RL1 (green), TM7 (blue), RL2 (green), and TM8 (yellow) of the GltPh structure (Yernool et al., 2004). The GltPh amino acid residues homologous to the ones mutated in EAAC1 in this study (see Fig. 1 A) are shown in red (numbering according to the EAAC1 sequence was used). All the residues mutated here (except E373, which is homologous to Q318 in GltPh) are conserved between EAAC1 and GltPh (Fig. 1 A). Bound glutamate is shown in yellow and was fit by eye into the presumed substrate binding pocket of the GltPh structure, with the γ-carboxylate pointing toward the side chain of R446 (blue). This bound glutamate in the GltPh structure demonstrates the global positioning of the bound substrate with respect to other structural elements of the transporter, but should not be considered the correct positioning. Orange residues denote acidic amino acids mutated in previous studies (Ryan et al., 2004; Tao et al., 2006). (C) Simulation of experimental data based on the model shown in A. Left top panel, glutamate induced anion current under exchange mode; right top, simulated $1/\tau$ versus $[Na^+]$ plot; left bottom, I_{steady}-$[Na^+]$ relationship; right bottom, I_{fast}-$[Na^+]$ (solid line) and I_{slow}-$[Na^+]$ (dotted line) relationships. The following parameters were used for all simulations: K_{Na1} = 200 mM, K_s = 300 μM, the forward rate constant for the slow phase was set to 0.3 s^{-1}, the backward rate was set to 0.5 s^{-1}, K_{Na2} = 250 mM. Glutamate and Na^+ binding reactions were assumed to be in rapid preequilibrium with respect to the slow conformational change. The relative conductance values for each state used in the calculations are shown in Fig. 7 A. The time dependence of the anion current was calculated by numerical integration of the rate equations pertaining to the model in Fig. 7 A. The $[Na^+]$ dependencies of the current components were calculated using Eqs. 2 and 4. I_{slow} was obtained by subtracting I_{steady}-I_{fast}.

this finding indicates that the rate of the slow current rising phase is limited by a process other than sodium binding, possibly a glutamate-induced conformation change (Larsson et al., 2004), as proposed earlier (Watzke et al., 2001).

If D439 does not form part of the Na^+ binding site, where could this binding site be located? We hypothesize that instead of D439, the bound substrate interacts with Na^+ and forms part of the Na^+ binding site. This hypothesis is consistent with our observation of impaired Na^+ binding to the glutamate-bound form of $EAAC1_{D439N}$, but not to the aspartate-bound form. In this model the D439N exchange leads to an altered interaction of glutamate with the transporter, impairing its ability to coordinate Na^+. This model is also consistent with our finding of negative cooperativity between glutamate and Na^+ in the mutant transporter, i.e., glutamate binds with lower apparent affinity to the transporter in the presence of Na^+ than in its absence. This interpretation would also be consistent with recent findings of the Kanner group, showing that the nature of the bound cation influences the affinity of the transporter for the amino acid substrate (Menaker et al., 2006). The amino acid substrate contributing a liganding atom to a Na^+ binding site has recently been shown for a bacterial leucine transporter, LeuT (Yamashita et al., 2005). In this transporter one of the α-carboxylate atoms of the substrate leucine serves as one of the six ligands of the bound Na^+ ion. It can be speculated that the α-carboxylate group of the acidic amino acid serves a similar function in glutamate transporters.

We have recently proposed that Na^+ binding to the glutamate-free transporter form takes place near the center of the hydrophobic core of the transporter (Tao et al., 2006). Specifically, we have identified an aspartate residue in position 367 to be involved in this binding process. In the GltPh structure the side chain of D367 is localized far apart from that of D439 (~18 Å) and the α-carboxylate of the substrate (~11 Å), as shown in Fig. 7 B (D367 depicted in orange space fill). Consistently, the D367N mutation had its major effect on the affinity of the empty transporter for Na^+, and not on the affinity

of the glutamate-bound form for Na^+. In agreement with this, the apparent affinity of the empty transporter for Na^+ was almost unaffected by the D439N mutation (Table I). Considering all the evidence, a picture emerges in which D367 is involved in binding of Na^+ to the empty transporter and E373 is the protonation site for the cotransported proton.

The D439N Mutation Converts Glutamate into a Partial Inhibitor of the Anion Conductance

The pharmacology of the glutamate transporter is changed by the D439N amino acid exchange. Whereas aspartate and TBOA have similar activities as in the wild-type protein, glutamate is converted into a partial inhibitor of the $EAAC1_{D439N}$ anion conductance, with properties of both full competitive inhibitors and activating substrates. PDC, which is a transported substrate in EAAC1 and activates the anion conductance, is converted to an inhibitor of the anion conductance in $EAAC1_{D439N}$ (Fig. 6). A similar observation was made for THA. However, in contrast to PDC, THA can still activate some anion current, as evidenced by the outward current overshoot after rapid application of THA (Fig. 6). We interpret this result such that THA initially inhibits the leak anion conductance (fast phase), leading to the peak of the outward current, and subsequently activates inward anion current (slow phase). However, in contrast to glutamate as the substrate, this inward anion current is not large enough to overcome the initial inhibition of the leak anion current. We can exclude the possibility that I_{fast} is caused by dissociation of Na^+ into the cytosol because this phase is equally present in the forward transport mode and in the homoexhange mode, which prevents intracellular Na^+ dissociation.

The Anion Conductance of $EAAC1_{D439N}$ Is Modulated by Na^+ and Glutamate Binding

Our data on $EAAC1_{D439N}$ show that glutamate binding does not immediately activate the substrate-dependent anion conductance, but it initially inhibits the leak anion conductance (Fig. 2). Thus, the unitary conductance of the Na^+/glutamate-bound state of the transporter must be smaller than that of the Na^+-bound state in the absence of glutamate, although it is not zero. A model that can explain the experimental data is shown in Fig. 7 A. In this model, the anion conductance of the transporter is modulated as EAAC1 moves through individual states of the transport cycle. We have estimated the unitary conductances of these individual states, G_i, relative to the conductance of the fully loaded transporter state, $T'Na_2S$ ($G_{rel} = G_i/G_{T'Na2S}$). This fully loaded state has the highest relative conductance in $EAAC1_{WT}$. However, in $EAAC1_{D439N}$ the unitary conductance of this state is lower than that of the TNa state, which has a G_{rel} of 1.2. The relative conductance values for each state are listed in Fig. 7 A. Using these parameters and assuming that the rate-limiting step is the transition from TNaS to T'NaS, which precedes Na^+ binding, we can quantitatively describe the time dependence of the glutamate-induced anion current in $EAAC1_{D439N}$, as well as the [Na^+] dependence of the individual current phases (Fig. 7 C). The parameters used for the calculations are listed in Table I. The model also quantitatively describes the measured $1/\tau$-[Na^+] relationship, predicting a small decrease of $1/\tau$ with increasing [sodium]. This behavior is expected for a rate-limiting step followed by a fast Na^+ binding reaction (Eq. 1, Appendix). The estimated relative conductance values for the individual transporter states directly show that the binding of Na^+, but not binding of glutamate, gates the $EAAC1_{D439N}$ anion conductance, as was suggested previously from indirect kinetic evidence obtained for wild-type EAAC1 (Watzke et al., 2001).

For $EAAC1_{WT}$, the ratio of relative unitary conductance of state TNa and $T'Na_2S$ in Fig. 7 A was estimated as 0.25, about fivefold lower than that of the mutant transporter. Therefore, mutations in position D439 directly influence the intrinsic anion conducting properties of the transporter, without fully abolishing its anion conductance. Similar behavior was demonstrated previously for a transporter with the mutation analogous to D112A in EAAT1 (Ryan et al., 2004) (corresponding to D83 in EAAC1), which, like $EAAC1_{D439N}$, shows an increased leak conductance relative to the substrate-activated conductance. It was proposed that D112 has the function of a gate for the anion conducting pathway. In the crystal structure of GltPh this amino acid residue is localized at the cytoplasmic end of TM3. Other residues in the cytoplasmic half of TM2 were also implicated in the anion conducting pathway. Because mutations to D439, which is localized at the extracellular end of TM8 far removed from D83 (Fig. 7 C), modulate the anion conductance, it is likely that D439 is not directly associated with the anion conducting pathway, and therefore modulates the anion conductance through an indirect mechanism by changing the conformation of the protein. Alternatively, D439 could be localized near the extracellular mouth of the anion permeation pathway.

In summary, the negatively charged amino acid residue D439 is important for various aspects of the normal function of EAAC1. Neutralization of this residue impairs Na^+ binding to the glutamate-bound form of the transporter dramatically and changes the pharmacology of the transporter, converting transported substrates into inhibitors. Two other conserved charged amino acid residues, E373 and D454, appear not to be involved in the coordination of Na^+ ions by the glutamate-bound transporter. We propose that D439, in cooperation with the bound substrate, controls the affinity of EAAC1 for one of the cotransported Na^+ ions.

While this work was under revision, a structure of GltPh with two bound Tl^+ ions was published (Boudker

et al., 2007). In this structure one of the two Tl^+ ions (which may be analogous to the Na^+ ion bound to the glutamate-bound transporter) is bound to a site that is close in space to the amino acid substrate binding site, but not in direct contact. This confirms our conclusion that D439 does not directly coordinate the Na^+ ion. Based on this structure, we speculate that the D439N mutation interferes with the glutamate-induced closure of reentrant-loop 2 (RL2), thus disrupting the interaction of the transporter with Na^+. The second Tl^+ ion (which may be analogous to the Na^+ ion bound to the glutamate-free transporter) is bound at a site involving the residue of GltPh analogous to D454 in EAAC1. This finding confirms our conclusion that D454 and D373 do not contribute to Na^+ binding to the glutamate-bound transporter.

APPENDIX

The model shown in Fig. 7 A is a simplified transport model that allows us to quantify the most important observations made for the $EAAC1_{D439N}$ transporter, by performing simulations and comparing them to the experimental data. The model does not include proton-dependent reactions and the third Na^+ binding step, because it is not known in which sequence these steps occur with respect to other partial reactions. Furthermore, we assume that the anion-conducting states are on the main kinetic pathway through the transport cycle, and not connected through side reactions, as proposed in some previous reports (Wadiche and Kavanaugh, 1998, Grewer et al., 2000). Considering these simplifications, it is unlikely that the model can explain all the experimental data available on EAAC1, but it describes the key kinetic features found in the $EAAC1_{D439N}$ transporter very well (Fig. 7 C). According to this model, the relaxation rate for the rise of the current, $1/\tau_{slow}$ (slow step in Fig. 7 A, red), can be expressed as follows:

$$\frac{1}{\tau_{rise}} = k_1 + k_{-1}\frac{K_{N2}}{[Na^+] + K_{N2}}. \quad (1)$$

Here, k_1 and k_{-1} are the rate constants for the rate limiting transitions TNaS→T'NaS and T'NaS→TNaS, respectively, and K_{N2} is the dissociation constant of the sodium ion from its site on T'NaS. The following assumptions were made: (a) the glutamate concentration is saturating, leading to saturation of the initial Na^+ binding step to the empty transporter; and (b) binding of glutamate, the initial Na^+ ion, and the final Na^+ ion are in rapid preequilibrium with respect to the transition TNaS↔T'NaS. This equation shows that $1/\tau_{slow}$ is either $[Na^+]$ independent ($k_1 >> k_{-1}$), or it decreases with increasing $[Na^+]$.

The steady-state anion current amplitudes of the transporters were calculated as outlined in the following paragraphs. The $[Na^+]$ dependence of the fast phase of the current was approximated as:

$$I_{fast} \approx G_{TNa}\frac{[Na^+]}{[Na^+] + K_{N1}} - G_{TNaS}\frac{[Na^+]}{[Na^+] + K_{app1}} \quad (2)$$

$$\text{with } K_{app1} = K_{N1}\frac{K_S}{[S] + K_S}. \quad (3)$$

Here, K_{N1} is the dissociation constant of Na^+ from the empty transporter form and K_S is the intrinsic dissociation constant of the amino acid substrate (S). G_i denotes the relative conductance of the respective state (see model in Fig. 7 A).

The steady-state current was described with the following expression:

$$I_{steady} \approx G_{TNa}\frac{[Na^+]}{[Na^+] + K_{N1}} - \frac{\frac{[Na^+]}{K_{N2}}\left(G_{TNaS}K_{N2} + G_{TNa2S}[Na^+]\right)}{\frac{[Na^+]^2}{K_{N2}} + [Na^+]\left(\frac{K_S + [S]}{[S]}\right) + K_{N1}\frac{K_S}{[S]}}. \quad (4)$$

The slow component of the current, I_{slow}, was obtained by subtraction of I_{fast} from I_{steady}.

The time dependence of the anion current of $EAAC1_{D439N}$ was calculated by numerical integration of the differential equations pertaining to the kinetic scheme shown in Fig. 7 A. Each state in the reaction sequence was assigned a relative conductance, as illustrated in Fig. 7 A. For these calculations, and the calculations from Eqs. 2–4, results were multiplied by an arbitrary scaling factor to be compared with actual measured currents. This scaling factor accounts for quantities such as number of transporters under observation and electrochemical driving force not included in Eqs. 2–4. The kinetic model shown in Fig. 7 A contains 10 variable parameters. Some of these parameters, such as the K_{N1} value for Na^+ binding to the empty transporter, and the K_S for substrate binding are well defined. For both of these values we can give a confidence interval of about ± 20%. In contrast, K_{N2} is not well defined in the numerical simulation and changes in K_{N2} from 100 to 300 mM do not affect the outcome of the simulations dramatically. It is evident that the forward rate constant for the slow step (k_1), the backward rate for the slow step (k_{-1}), and K_{N2} are interdependent. Therefore, K_{N2} will depend on the ratio of k_1/k_{-1}. Although this ratio can theoretically be determined from the data shown in Fig. 5 A and Eq. 1, the quality of this data, together with the small effect of $[Na^+]$ on $1/\tau_{slow}$ renders this determination difficult. However, a value that is well defined is the sum of (k_1 + k_{-1}), which is given by the apparent rate of the slow current rise.

We thank Dr. T. Rauen for providing the EAAC1 cDNA, and Dr. K. Fendler for helpful comments and suggestions regarding this work.

This work was supported by grants of the National Institutes of Health R01-NS049335-02, and the Deutsche Forschungsgemeinschaft GR 1393/2-2,3 to C. Grewer and by the American Heart Association 0525485B to Z. Tao.

Olaf S. Andersen served as editor.

Submitted: 10 October 2006
Accepted: 7 March 2007

REFERENCES

Arriza, J.L., S. Eliasof, M.P. Kavanaugh, and S.G. Amara. 1997. Excitatory amino acid transporter 5, a retinal glutamate transporter coupled to a chloride conductance. *Proc. Natl. Acad. Sci. USA.* 94:4155–4160.

Bendahan, A., A. Armon, N. Madani, M.P. Kavanaugh, and B.I. Kanner. 2000. Arginine 447 plays a pivotal role in substrate interactions in a neuronal glutamate transporter. *J. Biol. Chem.* 275:37436–37442.

Bergles, D.E., A.V. Tzingounis, and C.E. Jahr. 2002. Comparison of coupled and uncoupled currents during glutamate uptake by GLT-1 transporters. *J. Neurosci.* 22:10153–10162.

Billups, B., D. Rossi, and D. Attwell. 1996. Anion conductance behavior of the glutamate uptake carrier in salamander retinal glial cells. *J. Neurosci.* 16:6722–6731.

Boudker, O., R.M. Ryan, D. Yernool, K. Shimamoto, and E. Gouaux. 2007. Coupling substrate and ion binding to extracellular gate of a sodium-dependent aspartate transporter. *Nature.* 445:387–393.

Danbolt, N.C., G. Pines, and B.I. Kanner. 1990. Purification and reconstitution of the sodium and potassium-coupled glutamate transport glycoprotein from rat brain. *Biochemistry.* 29:6734–6740.

Danbolt, N.C., J. Storm Mathisen, and B.I. Kanner. 1992. A sodium and potassium coupled L glutamate transporter purified from rat brain is located in glial cell processes. *Neuroscience.* 51:295–310.

Davis, K.E., D.J. Straff, E.A. Weinstein, P.G. Bannerman, D.M. Correale, J.D. Rothstein, and M.B. Robinson. 1998. Multiple signaling pathways regulate cell surface expression and activity of the excitatory amino acid carrier 1 subtype of Glu transporter in C6 glioma. *J. Neurosci.* 18:2475–2485.

Fairman, W.A., R.J. Vandenberg, J.L. Arriza, M.P. Kavanaugh, and S.G. Amara. 1995. An excitatory amino-acid transporter with properties of a ligand-gated chloride channel. *Nature.* 375:599–603.

Gendreau, S., S. Voswinkel, D. Torres-Salazar, N. Lang, H. Heidtmann, S. Detro-Dassen, G. Schmalzing, P. Hidalgo, and C. Fahlke. 2004. A trimeric quaternary structure is conserved in bacterial and human glutamate transporters. *J. Biol. Chem.* 279:39505–39512.

Grewer, C., P. Balani, C. Weidenfeller, T. Bartusel, Z. Tao, and T. Rauen. 2005. Individual subunits of the glutamate transporter EAAC1 homotrimer function independently of each other. *Biochemistry.* 44:11913–11923.

Grewer, C., N. Watzke, T. Rauen, and A. Bicho. 2003. Is the glutamate residue Glu-373 the proton acceptor of the excitatory amino acid carrier 1? *J. Biol. Chem.* 278:2585–2592.

Grewer, C., N. Watzke, M. Wiessner, and T. Rauen. 2000. Glutamate translocation of the neuronal glutamate transporter EAAC1 occurs within milliseconds. *Proc. Natl. Acad. Sci. USA.* 97:9706–9711.

Larsson, H.P., A.V. Tzinqounis, H.P. Koch, and M.P. Kavanaugh. 2004. Fluorometric measurements of conformational changes in glutamate transporters. *Proc. Natl. Acad. Sci. USA.* 101:3951–3956.

Jorgensen, P.L., and P.A. Pedersen. 2001. Structure-function relationships of Na^+, K^+, ATP, or Mg^{2+} binding and energy transduction in Na,K-ATPase. *Biochim. Biophys. Acta.* 1505:57–74.

Kanai, Y., and M.A. Hediger. 1992. Primary structure and functional characterization of a high-affinity glutamate transporter. *Nature.* 360:467–471.

Kanner, B.I., and A. Bendahan. 1982. Binding order of substrates to the sodium and potassium ion coupled L-glutamic acid transporter from rat brain. *Biochemistry.* 21:6327–6330.

Kavanaugh, M.P., A. Bendahan, N. Zerangue, Y. Zhang, and B.I. Kanner. 1997. Mutation of an amino acid residue influencing potassium coupling in the glutamate transporter GLT-1 induces obligate exchange. *J. Biol. Chem.* 272:1703–1708.

Koch, H.P., and H.P. Larsson. 2005. Small-scale molecular motions accomplish glutamate uptake in human glutamate transporters. *J. Neurosci.* 25:1730–1736.

Levy, L.M., O. Warr, and D. Attwell. 1998. Stoichiometry of the glial glutamate transporter GLT-1 expressed inducibly in a Chinese hamster ovary cell line selected for low endogenous Na^+-dependent glutamate uptake. *J. Neurosci.* 18:9620–9628.

Meier, T., P. Polzer, K. Diederichs, W. Welte, and P. Dimroth. 2005. Structure of the rotor ring of F-type Na^+-ATPase from *Ilyobacter tartaricus. Science.* 308:659–662.

Menaker, D., A. Bendahan, and B.I. Kanner. 2006. The substrate specificity of a neuronal glutamate transporter is determined by the nature of the coupling ion. *J. Neurochem.* 99:20–28.

Murata, T., I. Yamato, and Y. Kakinuma. 2005. Structure and mechanism of vacuolar Na^+-translocating ATPase From *Enterococcus hirae. J. Bioenerg. Biomembr.* 37:411–413.

Pines, G., N.C. Danbolt, M. Bjoras, Y. Zhang, A. Bendahan, L. Eide, H. Koepsell, J. Storm Mathisen, E. Seeberg, and B.I. Kanner. 1992. Cloning and expression of a rat brain L glutamate transporter. *Nature.* 360:464–467.

Pines, G., Y. Zhang, and B.I. Kanner. 1995. Glutamate 404 is involved in the substrate discrimination of GLT-1, a (Na^+ + K^+)-coupled glutamate transporter from rat brain. *J. Biol. Chem.* 270:17093–17097.

Ryan, R.M., A.D. Mitrovic, and R.J. Vandenberg. 2004. The chloride permeation pathway of a glutamate transporter and its proximity to the glutamate translocation pathway. *J. Biol. Chem.* 279:20742–20751.

Seal, R.P., Y. Shigeri, S. Eliasof, B.H. Leighton, and S.G. Amara. 2001. Sulfhydryl modification of V449C in the glutamate transporter EAAT1 abolishes substrate transport but not the substrate-gated anion conductance. *Proc. Natl. Acad. Sci. USA.* 98:15324–15329.

Shimamoto, K., B. Lebrun, Y. Yasuda-Kamatani, M. Sakaitani, Y. Shigeri, N. Yumoto, and T. Nakajima. 1998. DL-threo-β-benzyloxyaspartate, a potent blocker of excitatory amino acid transporters. *Mol. Pharmacol.* 53:195–201.

Storck, T., S. Schulte, K. Hofmann, and W. Stoffel. 1992. Structure, expression, and functional analysis of a Na+-dependent glutamate/aspartate transporter from rat brain. *Proc. Natl. Acad. Sci. USA.* 89:10955–10959.

Tanaka, K., K. Watase, T. Manabe, K. Yamada, M. Watanabe, K. Takahashi, H. Iwama, T. Nishikawa, N. Ichihara, T. Kikuchi, et al. 1997. Epilepsy and exacerbation of brain injury in mice lacking the glutamate transporter GLT-1. *Science.* 276:1699– 1702.

Tao, Z., Z. Zhang, and C. Grewer. 2006. Neutralization of the aspartic acid residue Asp-367, but not Asp-454, inhibits binding of Na^+ to the glutamate-free form and cycling of the glutamate transporter EAAC1. *J. Biol. Chem.* 281:10263–10272.

Toyoshima, C., and G. Inesi. 2004. Structural basis of ion pumping by Ca^+-ATPase of the sarcoplasmic reticulum. *Annu. Rev. Biochem.* 73:269–292.

Wadiche, J.I., J.L. Arriza, S.G. Amara, and M.P. Kavanaugh. 1995. Kinetics of a human glutamate transporter. *Neuron*. 14:1019–1027.

Wadiche, J.I., and M.P. Kavanaugh. 1998. Macroscopic and microscopic properties of a cloned glutamate transporter/chloride channel. *J. Neurosci*. 18:7650–7661.

Watzke, N., E. Bamberg, and C. Grewer. 2001. Early intermediates in the transport cycle of the neuronal excitatory amino acid carrier EAAC1. *J. Gen. Physiol*. 117:547–562.

Yamashita, A., S.K. Singh, T. Kawate, Y. Jin, and E. Gouaux. 2005. Crystal structure of a bacterial homologue of Na1/Cl2-dependent neurotransmitter transporters. *Nature*. 437:215–223.

Yernool, D., O. Boudker, Y. Jin, and E. Gouaux. 2004. Structure of a glutamate transporter homologue from *Pyrococcus horikoshii*. *Nature*. 431:811–818.

Zerangue, N., and M.P. Kavanaugh. 1996. Flux coupling in a neuronal glutamate transporter. *Nature*. 383:634–637.